ISSN 1068-3755, Surface Engineering and Applied Electrochemistry, 2012, Vol. 48, No. 5, pp. 418–425. © Allerton Press, Inc., 2012.

Cu/Co–W Nanolayers Electrodeposited from Single Bath and Investigations of Their Nanohardness[1]

N. Tsyntsaru[a, b], S. Belevsky[b], H. Cesiulis[c], A. Dikusar[b], and J.-P. Celis[a]

[a] *Katholieke Universiteit Leuven, Dept. MTM, Kasteelpark Arenberg 44, B-3001 Leuven, Belgium*

[b] *Institute of Applied Physics, Academy of Sciences of Moldova, 5, Academiei str., Chisinau, MD-2028, Republic of Moldova*

[c] *Vilnius University, Dept. Phys. Chem., Naugarduko 24, Vilnius, LT-03225, Lithuania*

e-mail: ashra_nt@yahoo.com

Received January 24, 2012

Abstract—For the first time thick (~8 μm) Cu/Co–W multilayered coatings with individual layers ranging from 5 to 200 nm were electrodeposited from a single bath. The content of tungsten in rich-in Co–W layers was controlled by varying current densities in a citrate-borate bath. Continuous Multi-Cycle (CMC) nanoindentation technique was used to analyze mechanical properties of those deposits. Optical examination of the indented zone revealed the absence of cracks inside and outside the indentation area in the interval of the normal loads used. The hardness of Cu/Co–W multilayers varied with the bi-layer period and the electrodeposition parameters. The Cu/Co–W multilayers showed an increased hardness compared to that of Co–W coatings electrodeposited under the same conditions.

DOI: 10.3103/S1068375512050134

INTRODUCTION

Multilayers are attractive materials because a high density of interfaces induces physical and mechanical properties that differ from those of their bulk constituents. An electrodeposited multilayer thin film consists of alternating layers of at least two different materials with submicrometer layer thicknesses [1–4] or even in the nanometer range [5–9]. In most cases the co-depositing metals have quite different electrodeposition potentials. Frequently copper or gold are chosen as the noble metal, and an iron-group metal or its alloy—as an active metal [10]. Since both Cu(II) and Au(I) reduce easily, the concentration of these metals in the electrolyte is relatively low that enables electrodeposition of Cu or Au under mass-transport control. On the contrary, metals of the iron group are electrodeposited under kinetic control.

The electrodeposition of multilayers can be performed from a single bath under pulse current or pulse potential mode and the periodicity of the current or potential pulses triggers the alternated growth of the noble (active) metal layer at low (high) values of current or potential [10]. The electrodeposition of a number of multilayered coatings was reported, namely, of Cu/Ni, NiCo/Cu, Cu/Co, Cu/NiFe, Au/Co, Au/FeAu, and Cu/CoB/CoW(B)P [11–17]. Multilayered materials, tailored with a repetitive sequence of magnetic segments (e.g. iron group metals) interspaced by noble metal layers, display unique magnetic properties [18–20].

Functionally graded and periodic multilayer films often are investigated with intentions to use for applications as hard coating because of their superior properties which result from layered structure. Functionally graded multilayer coatings have been explored to improve toughness, hardness and the adhesion to the substrate [21]. The CMC nanoindentation test can be used to study delamination and the interfacial strength between layers [22].

The Co–W coatings electrodeposited from similar citrate baths potentially might be used as anticorrosive and wear resistance coatings [23, 24].

The aim of this study is to electrodeposit Cu/Co–W multilayers from a single bath and to investigate their mechanical properties.

EXPERIMENTAL

The electrodeposition of coatings was carried out in a standard 3-electrode cell. A graphite rod was used as an anode, a saturated Ag/AgCl electrode as the reference electrode. All potentials are reported versus the saturated Ag/AgCl reference electrode. Mild steel flat plates (working area 8 cm^2, composition 98.5 at % Fe, 0.5 at % C, 0.7 at % Si, others 0.3 at %) were used as substrates. Prior to electrodeposition, the substrates were mechanically polished. In order to improve the adhesion of the Cu/Co–W multilayers onto the substrates, the electrodeposition of a nickel seed layer was done from an electrolyte containing 1 M $NiCl_2$ and 2.2 M HCl at 3 A/dm^2 for 1 min. The electrodeposition conditions were controlled and monitored using a

[1] The article is published in the original.

Table 1. The compositions of electrolytes

No.	C_{CoSO_4}, M	$C_{Na_2WO_4}$, M	C_{CuSO_4}, M	$C_{C_6H_8O_7}$, M	$C_{Na_3C_6H_5O_7}$, M	$C_{H_3BO_3}$, M
Solution 1	0.2	0.2	0.002	0.04	0.25	0.65
Solution 2	–	–	0.002	0.04	0.25	0.65
Solution 3	0.2	0.2	–	0.04	0.25	0.65

PARSTAT 2273 system which was also used to record potentiodynamic polarization curves at a scan rate of 2 mV/s. In such experiments, a Cu wire was used as the working electrode.

Cu/Co–W multilayred coatings were electrodeposited from a single electrolyte (SOLUTION 1) at pH 6.7 and 60°C. The contents of all solutions used in this study are presented in Table 1.

The hardness of multilayers was determined by continuous multicycling nano-hardness tests (CSM Nano tester). The applied load was varied between 10 mN up to 200 mN without removing completely the indenter from the surface.

The surface roughness of as-deposited coatings was quantified by non-contact white light interferometry (WYKO NT 3300). The coating morphology was investigated by scanning electron microscopy (SEM) with Philips XL 30 FEG equipped with the energy dispersive x-ray spectroscope and a super-ultra-thin window. The composition of electrodeposited alloys reported in this study was calculated as the content of metallic phases. FIB (focus ion beam) cross-sections were made to reveal the multilayered structure.

Mechanical properties of the electrodeposited Cu/Co–W multilayers were compared to those of Co–W coatings electrodeposited at 3 A/dm^2 from a similar electrolyte as described elsewhere [24].

RESULTS AND DISCUSSIONS

Electrodeposition of Multilayered Coatings

The electrodeposition conditions were selected based on the potentiodynamic polarization curves recorded in three electrolytes whose compositions are presented in Table 1. The obtained potentiodynamic polarization curves are shown in Fig. 1. As it is seen, the electrodeposition of pure Cu starts at a more positive potential (approx. –0.1 V) than the electrodeposition of Co–W (approx. –0.5 V), and electrodeposition at reasonable rate is observed at potentials more negative than –0.7 V. In all multilayer deposition experiments described hereafter the current density used to electrodeposite Cu layer was kept as constant so that the electrodeposition potential would remain more positive than that for Co–W electrodeposition. The current densities for Co–W electrodeposition were varied. The pulse duration was chosen in such a way that the thickness of both the Cu-layers and the Co–W would be almost the same, namely 5–200 nm. The electrodeposition cycle contained also a pause needed to remove hydrogen bubbles from the cathode surface and to settle the values of pH in the pre-electrode space increased during the electrodeposition of Co–W layer due to hydroxyl ion production in the pre-cathode layer. To keep the constant pH values in course of the electrodeposition is very important when the electrodeposition of tungsten or molybdenum alloys is performed in deep recesses [25–27].

The following electrodeposition sequence was finalized to obtain multilayered coatings: (step 1) current pulse for the electrodeposition of Cu layer (duration t_{Cu} and amplitude i_{Cu}); (step 2) current pulse for the electrodeposition of the rich-in-Co-W layer (duration t_{CoW} and amplitude i_{CoW}); and (step 3) pause (duration t_{pause} and amplitude $i_{pause} = 0$). The parameters used for ectrodeposition of multilayers are summarized in Table 2. The potential response on the applied current path shown in Fig. 2 illustrates that the potential recorded during the galvanostatic growth of Cu sublayers remains sufficiently more positive than the one recorded during the growth of Co–W sublayers.

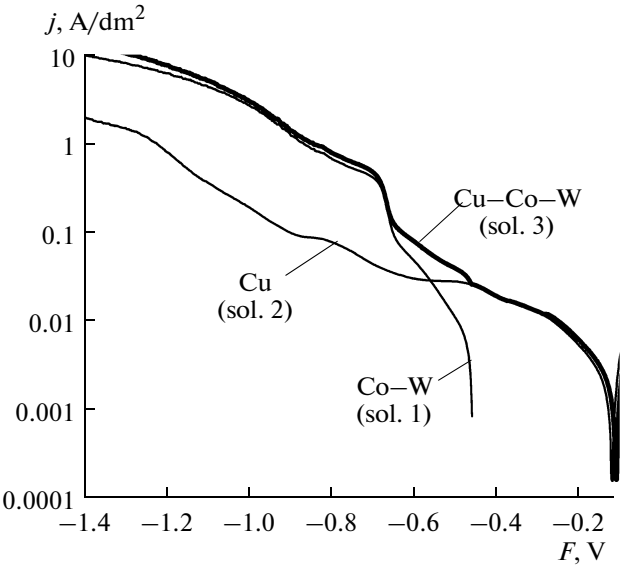

Fig. 1. Cathodic branches of potentiodynamic polarization curves recorded in Solutions 1–3.

Table 2. Conditions used for electrodeposition of Cu/Co–W multilayers and some coating characteristics obtained

No. of the plating conditions	t_{Cu}, s	i_{Cu}, A/dm^2	t_{CoW}, s	i_{CoW}, A/dm2	t_{pause}, s	Sublayer thickness, nm	Coating thickness, μm	Content of metallic elements, Co/W/Cu, at. %	Mean surface roughness R_a, nm
1	37.5	0.05	1.25	3	2.5	~ 5	10	76.2/19.0/4.8	110
2	1500		50	3	100	~ 200	10	61.6/18.7/19.7	853
3	45		2.4	2	12	~ 7	8	79.2/14.3/6.5	150
4	90		4.8	2	24	~ 12	7	71.9/16.8/11.3	201
5	45		3.2	1	16	~ 4.5	7	82.5/14.2/3.3	480

Structure of the Multilayered Coatings

Figure 3 presents the FIB-analysis of multilayers electrodeposited under the plating condition no. 2 and indicated in Table 2. The dark layers are copper sublayers and the grey ones are Co–W sublayers.

The FIB-analysis allows to estimate the thickness of the sublayers and to derive the current efficiency. As is shown in Fig. 3, the thickness of each layer was determined as ~200 nm and this values is close to the calculated one using Faraday's law (equation). Multilayers with thick sublayers of 200 nm grow uniformly till a total thickness does not exceed 1–2 μm (Figs. 3c and 3d). When the coatings become thicker, the uniformity of the thickness of individual layers is lost probably due to the following reasons: (1) the interfacial roughness and/or substitutional disorder (i.e. mixing of the adjacent metal atoms at the interface) that is always present in experiments [28]; (2) the influence of hydrogen evolution leading to the intensification of roughness [29]; (3) Cu(II) electroreduction from citrate solutions occurs under diffusion control [30]. All these peculiarities might cause the sequential decrease in the thickness of layers.

The last hypothesis can be qualitatively explained in the following way. Cu sublayers are electrodeposited under diffusion that limits current control (Fig. 1), therefore the concentration of Cu(II) complexes at the cathode surface is $[Cu(II)]_{x=0} = 0$. During electrodeposition of the rich-in-Co–W layer, Cu electroreduction occurs also at $[Cu(II)]_{x=0} = 0$, but with the gradually decreasing value of the concentration fluxion $(\partial[Cu(II)]/\partial x)_{x=0}$. The partial current density for Cu electrodeposition (j_{Cu}) is proportional to this term, as below:

$$j_{Cu} = nFD_{Cu(II)}\left(\frac{\partial[Cu(II)]}{\partial x}\right)_{x=0}, \quad (1)$$

where $D_{[Cu(II)]}$ is the diffusion coefficient of Cu(II) species.

The decrease of the concentration fluxion with time under condition $[Cu(II)]_{x=0} = 0$ can be describe based on the Cottrell equation, and is expressed in a following way:

$$\left(\frac{\partial[Cu(II)]}{\partial x}\right)_{x=0} = \frac{[Cu(II)]_0}{\sqrt{\pi D_{Cu(II)}}}, \quad (2)$$

where $[Cu(II)]_0$ is concentration in the bulk of electrolyte.

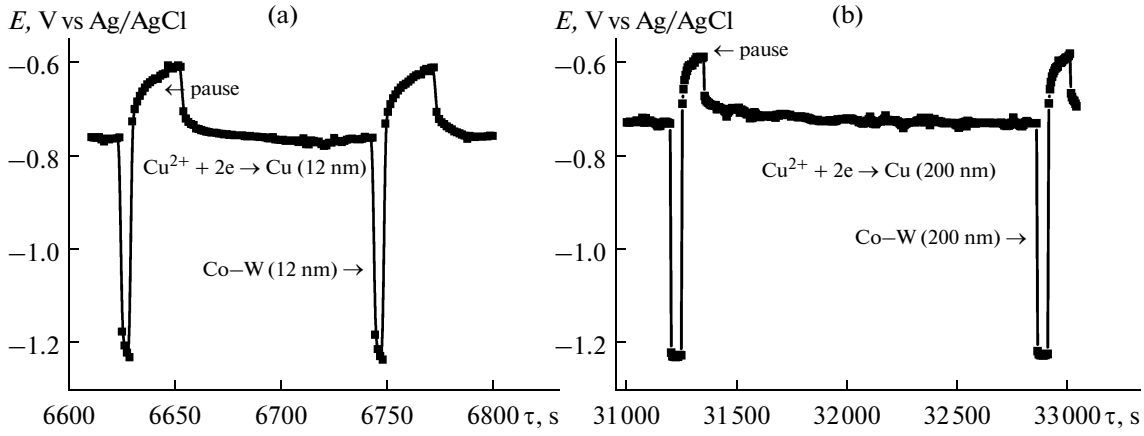

Fig. 2. Cathode potential changes during electrodeposition under conditions nos. 2 and 4 (see Table 2). Potentials are reported without ohmic drop compensation.

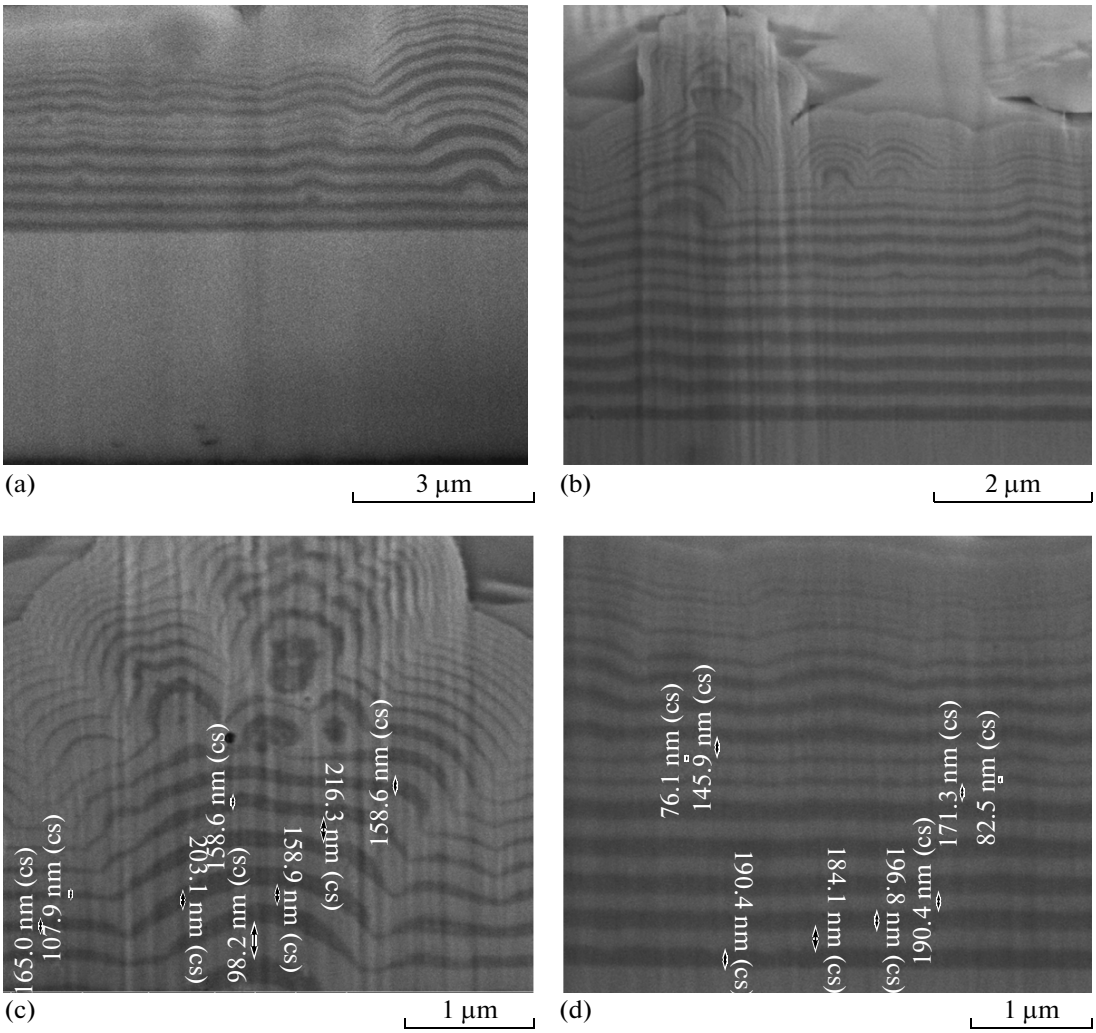

Fig. 3. SEM images taken on a FIB cross-section of a Cu/Co–W multilayer coating electrodeposited under the set of parameters 2 listed in Table 2. The (a, b, c) and (d) are the images taken in different spots of cross-section.

The decrease of the concentration fluxion results in the growing thickness of the diffusion layer during the pulse duration, because of the distance where concentration flux of $[Cu(II)] = [Cu(II)]_0$ becomes longer. Probably, during the pause time the concentration of Cu(II) at the cathode surface does not restore fully to its initial value but remains less than in the bulk of the electrolyte. Therefore, each subsequent deposition cycle starts at a gradually lower $[Cu(II)]_{x=0}$, which results in a lower partial current for Cu and thus in a sublayer thickness deviation.

Another reason is dealing with Cu electrodeposits obtained at limiting current density. In this case a relatively rough surface is formed, which results in widening the real surface area, thus causing a decrease in current density at constant current applied. Lowering of the Cu sublayer thickness appears more pronounced at a thicker initial sublayer thickness.

SEM images of multilayers electrodeposited under different conditions are shown in Fig. 4. The coatings differ in as-plated roughness (Table 2) and in surface inhomogeneities. The coatings deposited under condition no. 2 (Table 2), resulting in the highest sublayer thickness, have the highest roughness, whereas coatings deposited under other conditions indicated in Table 2 exhibit only "islands" of inhomogeneity. It is worth noting here that an intensified roughness is also obtained when the low current densities are applied for the electrodeposition of Co–W layers (condition no. 5).

Mechanical Behaviour of Cu/Co–W Multilayers

The nanohardness of Cu/Co–W multiyares was investigated by CMC nanoindentation. In CMC, the coatings are loaded up to a specific value, then unloaded and immediately re-loaded to a higher load at the same place; and a cyclic nanoindentation curve

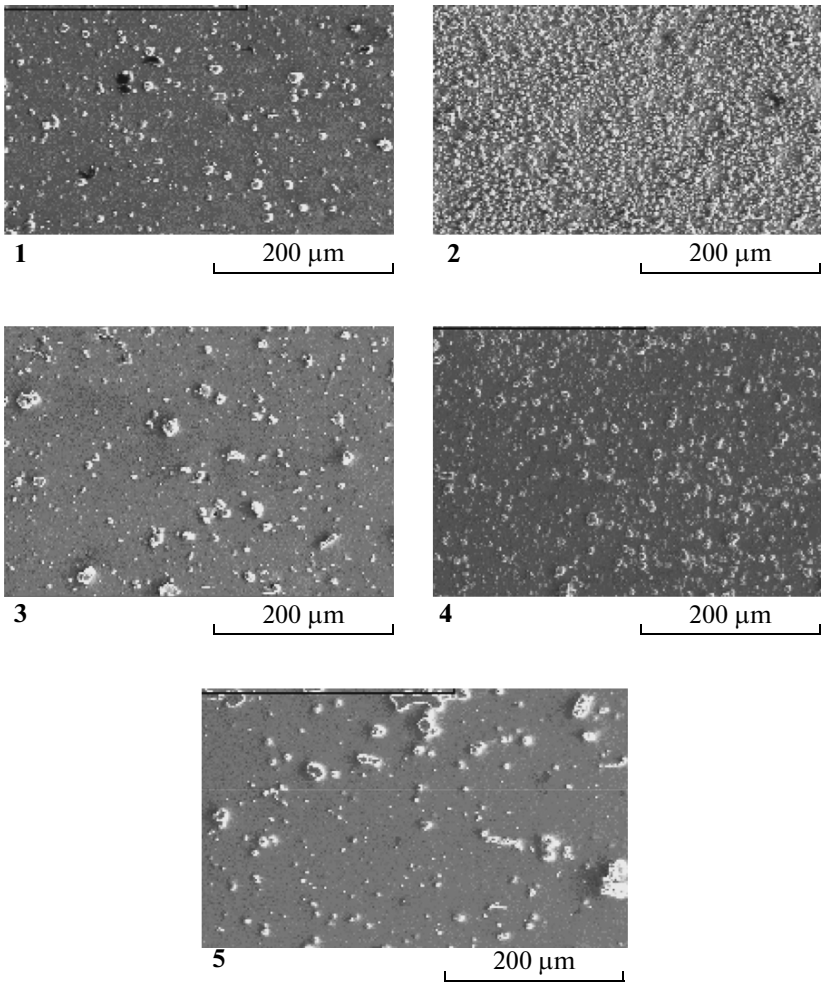

Fig. 4. SEM images of as-plated surfaces of Cu/Co–W multilayers. Numbers under images correspond to numbers of electrodeposition parameters listed in Table 2.

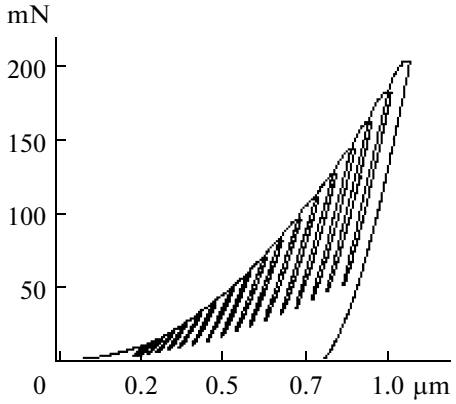

Fig. 5. Typical CMC loading nanoindentation test on Cu/Co–W multilayers.

is recorded. This method allows to check stability and crack initiation during continuous and high-speed loading. This test can be used to study buckling, delamination of the coating and the interfacial strength between the layers and the substrate. To understand the influence of the layered structure, 19 cycles were performed in one CMC test with the progressive loading from 10 mN up to 200 mN (Fig. 5). This allowed to keep the penetration depth not exceeding 10% of the coating thickness.

The topographies of the indented zone acquired by optical microscopy of the investigated coatings after CMC indentations are shown in Fig. 6, numbered respectively on the electrodeposition mode used. Several factors influence the hardness: the formation of cracks in the coating, properties of the material, indentation size, influence of the substrate effect and others [31]. As can be noticed from Fig. 6, the indentation imprints did not show any cracks, but such factors as tungsten content, hydrogen evolution, thick-

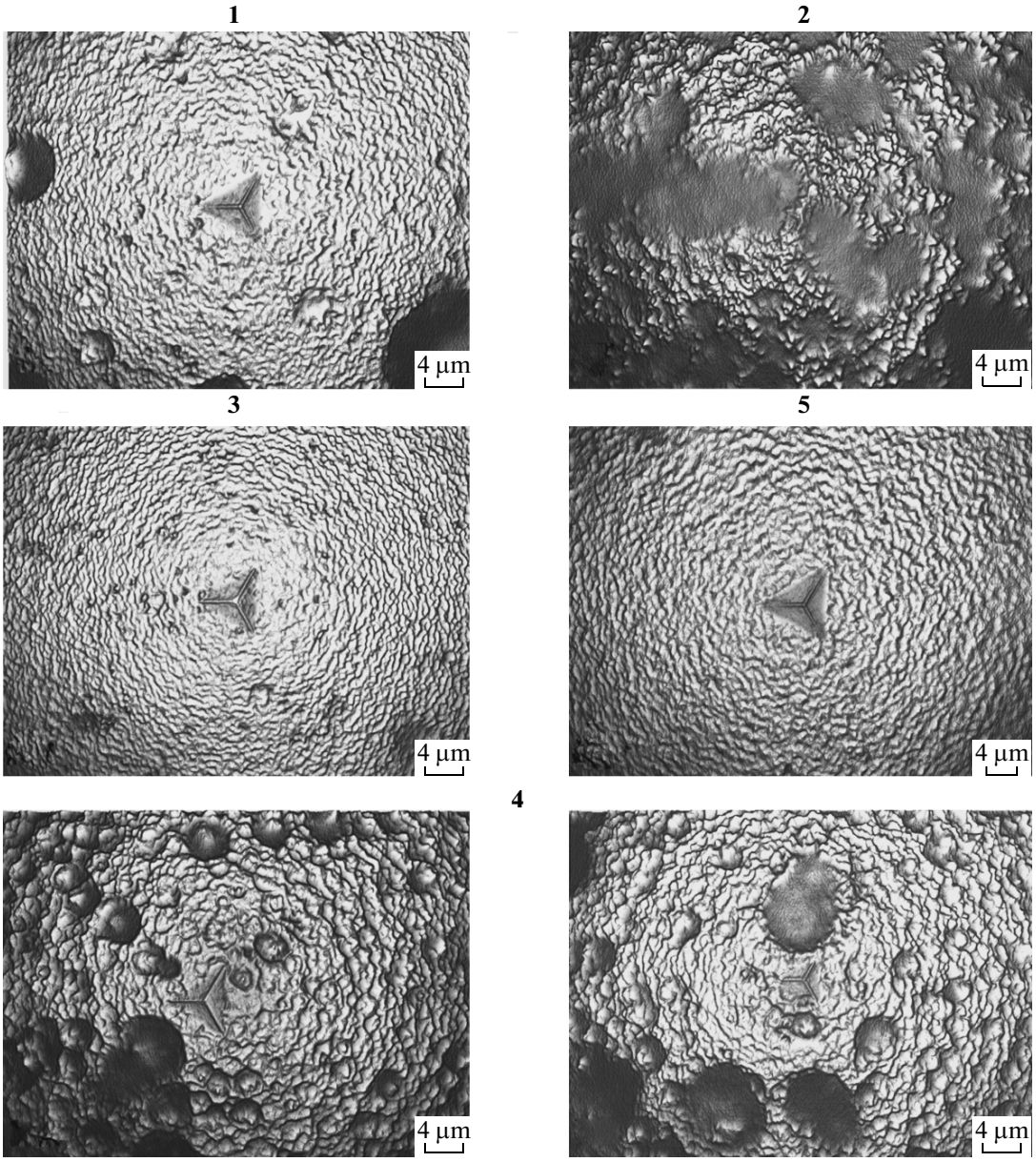

Fig. 6. Images of nanoindentation imprints of Cu/Co–W coatings electrodeposited under electrochemical conditions as shown in Table 2. Condition no. 4 can have different degrees of roughness and is presented by 2 images.

ness of sublayers do have effect on the resulting topography and hardness of the multilayered coating (Figs. 6 and 7).

Thus, a higher current density (3 A/dm^2, condition no. 1) applied for Co–W electrodeposition leads to a higher cathodic polarization and tungsten content in the multilayered coatings (Table 2). The presence of more tungsten in the coating results in higher hardness values (Fig. 7 graph **1**), but simultaneously it promotes a more intensive hydrogen bubbles formation (Fig. 6, image **1**). Increase of surface heterogeneities under condition no. 1 in comparison with electrodepostion under conditions nos. 3 and 5 leads to higher scattering values of hardness, which can be bigger or smaller than those for the Co–W ones (~9 GPa). Even, under the electodeposition condition no. 2, with the same current density as in no. 1, but with ~200 nm sublayers, the indentation cannot be carried out correctly, because of the extremely high roughness of the as-deposited Cu/Co–W coating. Increase of the thickness of sublayers requires longer deposition time, that leads to intensification of hydrogen evolution and roughness.

The negative influence of the increased sublayer thickness on the hardness of the investigated multilayers can be also noticed for the coatings electrodeposited under condition no. 4: coatings with ~12 nm sub-

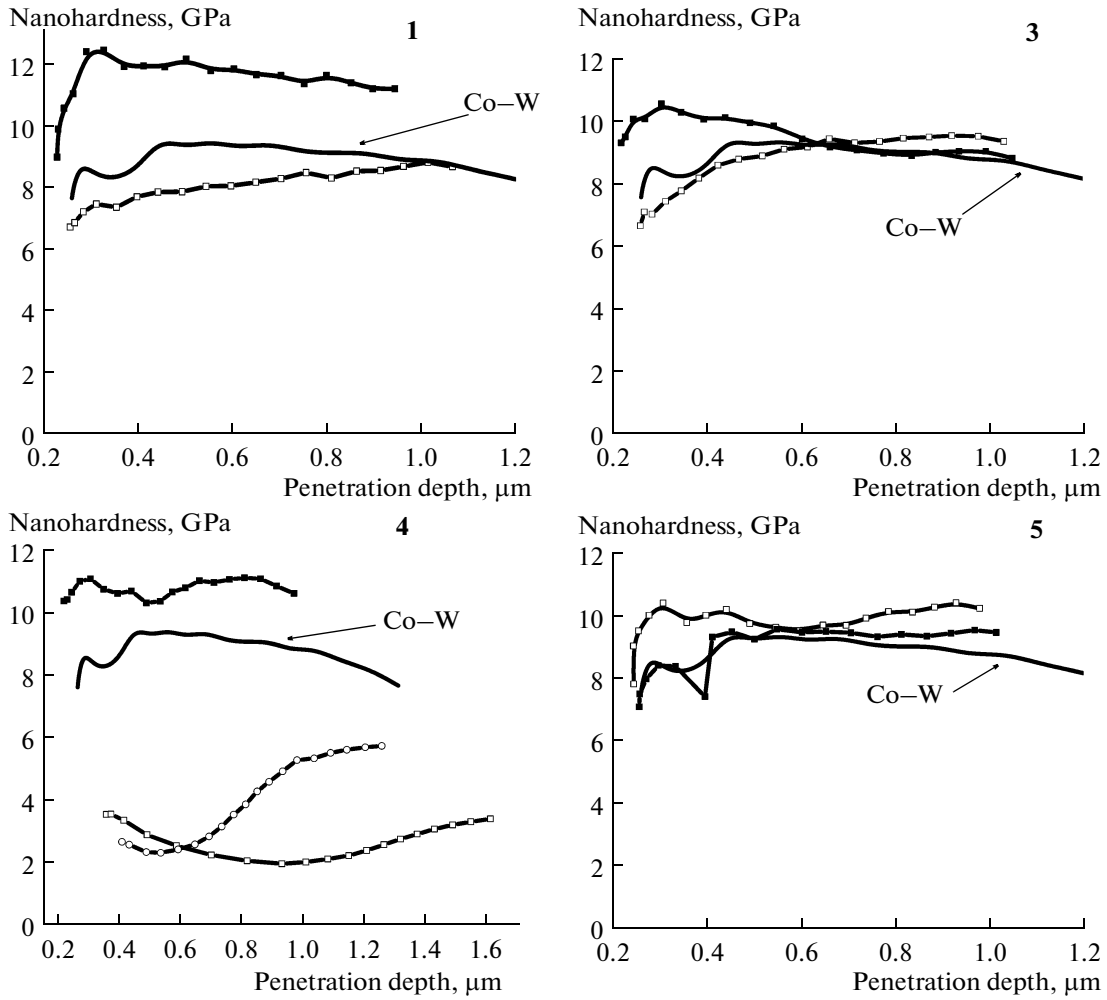

Fig. 7. Nanohardness measured by CMC method for the deposition conditions nos. 1, 3–5 (see Table 2). Different curves correspond to measurements at different spots on the coating.

layers have increased copper content and hence the hardness values can be very low (Fig. 7, graph **4**).

The remaining coatings electrodeposited under conditions nos. 3 and 5 are more uniform and their hardness varies within a narrower range. The scattering of the hardness values at small penetration depths (Fig. 7) can be due to the mixing of adjacent atoms at the interface of the upper layers of the coating. Nevertheless, for the majority of cases, the Cu/Co–W multilayers have better elastic recovery, which resulted in lower values of the penetration depth in comparison to those of Co–W coatings (Fig. 7). The hardness of Cu/Co–W coatings is close to or even exceeds the values obtained for the electrodeposited Co–W coatings.

CONCLUSIONS

The electrodeposition of Cu/Co–W multilayers was performed for the first time. The challenge of this study was to produce Cu/Co–W multilayers with a high total thickness of coatings and nanosized sublayers.

The mechanical properties of these Cu/Co–W multilayered coatings were compared with those of Co–W coatings electrodeposited from a similar bath. The hardness of Cu/Co–W multilayers varies with the electrodeposition parameters. The Cu/Co–W multilayers show, in most cases, an increase in hardness compared to that of Co–W coatings electrodeposited under the same conditions.

ACKNOWLEDGMENTS

This research was funded by the FP7 grants "NANOALLOY" (no. 252407), and "TEMADEP" (no. 247659) and also from the Research Council of Lithuania (grant no. MIP-134/2010-2011).

REFERENCES

1. Kirilova, I., Ivanov, I., and Rashkov, S.T., Anodic Behaviour of Composition Modulated Zn-Co Multilayers Electrodeposited from Single and Dual Baths., *J. Appl. Electrochem.*, 1998, vol. 28, pp. 637–1359.

2. Jensen, J.D., Gabe, D.R., and Wilcox, G.D., The Practical Realization of Zinc-Iron CMA Coatings, *Surf. Coat. Technol.*, 1998, vol. 105, pp. 240–250.
3. Chawa, G., Wilcox, G.D., and Gabe, D.R., Compositionally Modulated Zinc Alloy Coatings for Corrosion Protection, *Trans. IMF*, 1998, vol. 76, p. 117.
4. Kalantary, M.R., Wilcox, G.D., and Gabe, D.R., Alternate Layers of Zinc and Nickel Electrodeposited to Protect Steel, *Br. Corrosion J.*, 1998, vol. 33, pp. 197–201.
5. Herman, A.M., Mansour, M., Badri, V. et al., Deposition of Smooth Cu(In, Ga)Se_2 Films from Binary Multilayers, *Thin Solid Films*, 2000, vol. 74, pp. 361–362.
6. Pasa, A.A. and Schwarzacher W., Electrodeposition of thin Films and Multilayers on Silicon, *Phys. Stat. Sol.*, 1999, vol. 173, pp. 73–84.
7. Toth Kadar, E., Peter, L., Becsei, T., Toth, J., Pogany, L., Tarnoczi, T., Kamasa, P., Lang, G., Cziraki, A., and Schwarzacher, W., Preparation and Magnetoresistance Characteristics of Electrodeposited Ni-Cu Alloys and Ni–Cu/Cu Multilayers, *J. Electrochem. Soc.*, 2000, vol. 147, pp. 3311–3318.
8. Jyoko, Y., Kashiwabara, S., Hayashi, Y., and Schwarzacher, W., Preparation of Perpendicular Magnetization Co/Pt Nanostructures by Electrodeposition, *Electrochem. Solid Stat. Lett.*, 1999, vol. 2, pp. 67–69.
9. Ueda, Y., Houga, T., Zaman, H., and Yamada, A., Magnetoresistanc Effect of Co-Cu Nanostructure Prepared by Electrodeposition Method, *J. Solid Stat. Chem.*, 1999, vol. 147, pp. 274–280.
10. Davis, D., *Electrodeposition of Magnetic Nanowires and Nanotubes: Electrodeposition of Multilayered CoNiFe/Cu Nanowires and Nanotubes for Giant Magneto Resistance Sensing*, LAP Lambert Acad. Publ., 2010, p. 100.
11. Nabiyouni, G. and Schwarzacher, W., Growth, Characterization and Magnetoresistive Study of Electrodeposited Ni/Cu and Co-Ni/Cu Multilayers, *J. Cryst. Growth.*, 2005, vol. 275, nos. 1–2, pp. 1259–1262.
12. Gomez, E., Pane, S., and Valles, E., Electrodeposition of Co-Ni and Co-Ni-Cu Systems in Sulphate-Citrate Medium, *Electrochim. Acta*, 2005, vol. 51, p. 146.
13. Cziraki, T., Koteles, M., Peter, L., Kupay, Z., Padar, J., Pogany, L., Bakonyi, I., Uhlemann, M., Herrich, M., Arnold, B., Thomas, J., Bauer, H.D., and Wetzig, K., Correlation between Interface Structure and Giant Magnetore-sistance in Electrodeposited Co–Cu/Cu Multilayers, *Thin Solid Films*, 2003, vol. 433, pp. 237–242.
14. Chassaing, E., In situ Mass Changes and Stress Measurements in Cu/$Fe_{20}Ni_{80}$ Electrodeposited Multilayers, *J. Electrochem. Soc.*, 1997, vol. 144, pp. L328–L330.
15. Guan, M. and Podlaha, E.J., Electrodeposition of AuCo Alloys and Multilayers, *J. Appl. Electrochem.*, 2006, vol. 37, pp. 549–555.
16. Lucatero, S. and Podlaha, E.J., Influence of Citric and Ascorbic Acids on Electrodeposited Au/FeAu Multilayer Nanowires, *J. Electrochem. Soc.*, 2010, vol. 157, pp. D370–D375.
17. Hyo-Chol Koo, Sung Ki Cho, Oh Joong Kwon, Myung-Won Suh, Young Im, and Jae Jeong Kim, Improvement in the Oxidation Resistance of Cu Films by an Electroless Co-Alloy Capping Process., *J. Electrochem. Soc.*, 2009, vol. 156, pp. D236–D241.
18. Huang, Q. and Podlaha, E.J., Simulation of Pulsed Electrodeposition for Giant Magnetoresistance Fe-CoNiCu/Cu Multilayers, *J. Electrochem. Soc.*, 2004, vol. 151, pp. C119–126.
19. Meuleman, I.W.R.A., Roy, S., Peter, L., and Varga, I., Effect of Current and Potential Waveforms on Sublayer Thickness of Electrodeposited Copper-Nickel Multilayers, *J. Electrochem. Soc.*, 2002, vol. 149, pp. C479–C486.
20. Schwarzacher, W. and Lashmore, D.S., Giant Magnetoresistance in Electrodeposited Films, *IEEE Trans. Magn.*, 1996, vol. 32, pp. 3133–3153.
21. Lin, J., Moore, J.J., Moerbe, W.C., Pinkas, M., Mishra, B., Doll, G.L., and Sproul, W.D., Structure and Properties of Selected (Cr–Al–N, TiC–C, Cr–B–N) Nanostructured Tribological Coatings, *Int. J. Refract. Met. Hard Mater.*, 2010, vol. 28, pp. 2–14.
22. Bruno, P., Cicala, G., Losacco, A.M., and Decuzzi, P., Mechanical Properties of PECVD Hydrogenated Amorphous Carbon Coatings via Nanoindentation and Nanoscratching Technique, *Surf. Coat. Technol.*, 2004, vols. 180–181, pp. 259–264.
23. Tsyntsaru, N., Dikusar, A., Cesiulis, H., Celis, J.-P., Bobanova, Z., Sidel'nikova, S., Belevskii, S., Yapontseva, Y., Bersirova, O., and Kublanovskii, V., Tribological and Corrosive Characteristics of Electrochemical Coatings Based on Cobalt and Iron Superalloys, *Powder Metal. Metal Ceram.,* 2009, vol. 48, nos. 7–8, pp. 419–428.
24. Tsyntsaru, N., Belevsky, S., Dikusar, A., and Celis, J.-P., Tribological Behaviour of Electrodeposited Cobalt-tungsten Coatings: Dependence on Current Parameters, *Trans IMF*, 2008, vol. 86, no. 6, pp. 301–307.
25. Cesiulis, H. and Podlaha-Murphy, E.J., Electrolyte Considerations of Electrodeposited Ni-W Alloys for Micro Device Fabrication, *Mater. Sci. (Medziagotyra)*, 2003, vol. 9, no. 4, pp. 324–327.
26. Cesiulis, H., Xie, X.G., and Podlaha-Murphy, E., Electrodeposition of Co-W Alloys with P and Ni, *Mater. Sci. (Medziagotyra)*, 2009, vol. 15, no. 2, pp. 115–122.
27. Cesiulis, H., Tsyntsaru, N., Budreika, A., and Skridaila, N., Electrodeposition of CoMo and CoMoP Alloys from the Weakly Acidic Solutions, *Surf. Eng. Appl. Electrochem.*, 2010, vol. 46, no. 5, pp. 406–415.
28. Tsymbal, E.Y. and Pettifor, D.G., Perspectives of Giant Magnetoresistance, in *Solid State Physics*, Ehrenreich, H. and Spaepen, F., Eds., Acad. Press, 2001, vol. 56, pp. 113–237.
29. Gabe, D.R., The Role of Hydrogen in Metal Electrodeposition Processes, *J. Appl. Electrochem.*, 1997, vol. 27, no. 8, pp. 908–915.
30. Fundamental Aspects of Electrochemical Deposition and Dissolution, *Proc. Int. Symp.*, Matlosz, M., et al., Eds., 2000, vol. 99–33, p. 438.
31. Karimi, A., Wang, Y., Cselle, T., and Morstein, M., Fracture Mechanisms in Nanoscale Layered Hard Thin Films, *Thin Solid Films*, 2002, vols. 420–421, pp. 275–280.